

Evaluation of a Command Monitoring Concept for a V/STOL Research Aircraft

J. A. Schroeder*, E. Morales* and V. K. Merrick†
NASA Ames Research Center, Moffett Field, California

A simplex control system monitoring concept is described, which has the potential of rapidly detecting computer command failures (hardware or software) in fly-by-wire control systems. The concept has been successfully tested on a model of the NASA Vertical/Short Takeoff and Landing Research Aircraft in the Ames Research Center's Vertical Motion Simulator. The monitoring concept detected both slow and fast failures quickly enough to allow the pilot to make a safe recovery while performing landings on a destroyer-sized ship. The monitoring concept did not suffer from nuisance disconnects during the evaluations.

Introduction

NASA'S Vertical/Short Takeoff and Landing Research Aircraft (VSRA) is a YAV-8B Harrier that is currently being modified to provide in-flight data in support of research on V/STOL controls and displays. The culmination of this research program will be the identification and demonstration of a technology that will permit safe vertical landings on small ships operating in high seas and under conditions of poor visibility.

The VSRA control system uses the original YAV-8B mechanical control system augmented by a single-channel digital electronic subsystem. This subsystem can be engaged or disengaged from the mechanical system by the pilot. This electronic augmentation is designed to permit the evaluation of a wide variety of pilot command and stabilization modes in all the five controllable degrees of freedom of this aircraft.

The primary problem in designing a single-channel electronic control system for a single-seat aircraft is that of providing adequate safety in the event of a failure. In many of today's aircraft that are used for flight-control research, system failure problems are solved either by having a safety pilot monitor the single-channel system, or by using multiple computers in which a voting scheme is used to detect a failure (e.g., X-29). In the latter case, software failures are detected through the implementation of dissimilar coding in the computers. In today's single-seat production aircraft that depend on flight-control computers to either maintain safe operations or provide adequate handling qualities (e.g., F-18, F-16), redundant computation is employed. A typical arrangement of this type is in Ref. 1.

An example of a research aircraft flown at NASA Ames is the CH-47 variable stability helicopter, which has a safety pilot who monitors the system through full-authority controls backdriven by parallel actuators and nonredundant electronics.² Electronic hardover monitoring is accomplished by determining the parallel actuator's rate from position measurements. If the derived rate exceeds 80% of the maximum rate capability, the research system disengages (attitude parallel servo position measurements are filtered to minimize nuisance

disengagements).³ Another research aircraft flown at NASA Ames was the Augmentor Wing, which had a single computer driving servos in a parallel-series arrangement. A safety pilot and basic electronic monitoring, which examined normal and lateral accelerations and servo rates, checked system integrity.⁴

Achieving an acceptable level of failure monitoring in the VSRA will be more difficult, because the VSRA is very agile and will be expected to land in a very confined space in a severe environment. With the servo authorities proposed for the VSRA, simple calculations show that, in many cases, a failure must be detected and the reversion to the YAV-8B mechanical system effected in less than 1 s. This response time dictates that failure detection and system reversion be automatic. It is anticipated, using end-around and in-line techniques, that sensor and servo failures can be detected and reversion completed in less than two computer cycles (64 ms). The situation with regard to computer command failures is much less clear. Failures producing sudden large command changes can be detected easily and quickly, whereas others are slower and, therefore, difficult to detect in time to avert a disaster.

In this paper, a monitoring scheme for detecting any kind of computer command failure is described and applied to the VSRA. This scheme has been tested in a piloted, moving-based simulation that was generally aimed at evaluating the effects of VSRA servo and computer command failures. A description of the monitoring concept and the results of the control-system failure tests are given.

Aircraft System Description

The YAV-8B is a single-seat, transonic, light attack V/STOL aircraft powered by a single turbofan engine. The aircraft is similar to the AV-8A, but the YAV-8B has an improved inlet, a larger wing, reduced-splay front nozzles, and lift improvement devices under the fuselage. A three-view general arrangement drawing is shown in Fig. 1. The aircraft is being modified by installing two digital flight-control computers, two ring-laser gyro inertial measurement units (IMU), a servo control unit (SCU) to route computer commands to the appropriate servos (the SCU will also monitor servo hardware failures), and a set of servos to drive the throttle and nozzles.

A block diagram of the VSRA control and display system is shown in Fig. 2. Of particular note here is that one of the digital computers is used for control-law calculations and the other for monitoring the aircraft's dynamic response. Both computers receive inputs from the pilot and from the aircraft's sensors.

A complete description of the proposed control modes is given in Ref. 5. Briefly, these laws are based on a state-rate-feedback-implicit-model-follower (SRFIMF) approach.⁶ A

Presented as Paper 87-2535 at the AIAA Guidance, Navigation and Control Conference, Monterey, CA, Aug. 17-19, 1987; received June 22, 1987; revision received Oct. 18, 1987. Copyright © 1987 American Institute of Aeronautics and Astronautics, Inc. No copyright is asserted in the United States under Title 17, U.S. Code. The U.S. Government has a royalty-free license to exercise all rights under the copyright claimed herein for Governmental purposes. All other rights are reserved by the copyright owner.

*Aerospace Engineer, Flight Dynamics and Controls Branch. Member AIAA.

†Senior Research Engineer, Flight Dynamics and Controls Branch.

block diagram of the SRFIMF, appropriate to a second-order model, is shown in Fig. 3. The two gains K_x and $K_{\dot{x}}$ determine the natural frequency and damping of the model, the filter $A(s)$ compensates for the actuator dynamics, and the coupling gain K drives the poles of the aircraft toward zeros created in the feedback loops of the controller's structure. Thus, the closed-loop system has poles that are approximately in the same location as the poles of the desired model. The filter $A(s)$ also provides self-trimming (i.e., a step-disturbance produces no steady-state error), which is an essential feature for the application of the monitoring technique, as will be seen.

Figure 4 shows how the electronic control system is mechanized for a typical axis. It can be seen that the servo arrangement includes both a series and a parallel servo. The series servo in Fig. 4 is a position-command servo of high bandwidth and low amplitude. The parallel servos are low-fixed-rate, high-amplitude servos. The parallel servos provide a trim follow-up function to unload the series servos. This mechanization is cost effective, since the existing attitude trim and SAS servos will be used. The only servo modifications will be the addition of two series and two parallel servos for the throttle and nozzles. The amplitudes and rates of the servos, as well as the maximum control displacements available for all control axes, are given in Table 1. VSRA simulations at NASA Ames showed that the servo characteristics selected achieved desired performance of the research control modes, given in Table 2, for the environments in which the VSRA will operate.⁵ The pilot has to recover from, and monitoring effectiveness is dependent on, each of these control modes.

Monitoring System Requirements

Requirements Simulation

A previous simulation experiment established the performance requirements for the monitoring system. The tests in that study were designed to concentrate on simulating failures during shipboard landings, which is the most hazardous environment in which the VSRA will have to operate with the advanced control system. The most critical situation occurs

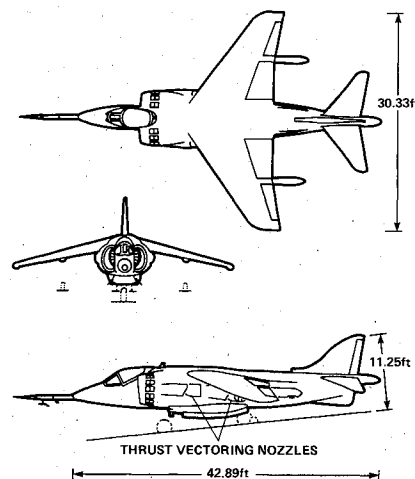


Fig. 1 YAV-8B Harrier.

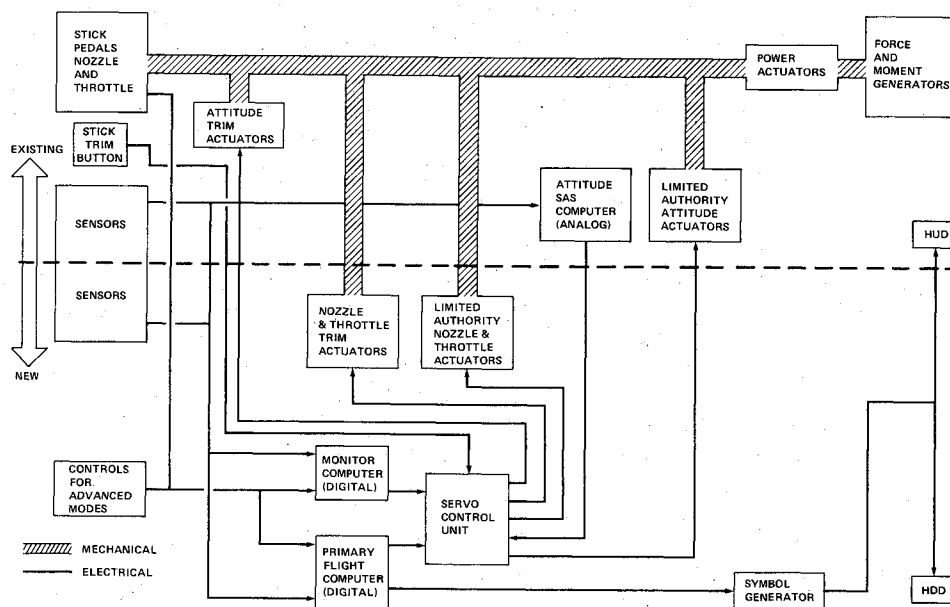


Fig. 2 VSRA control-display system.

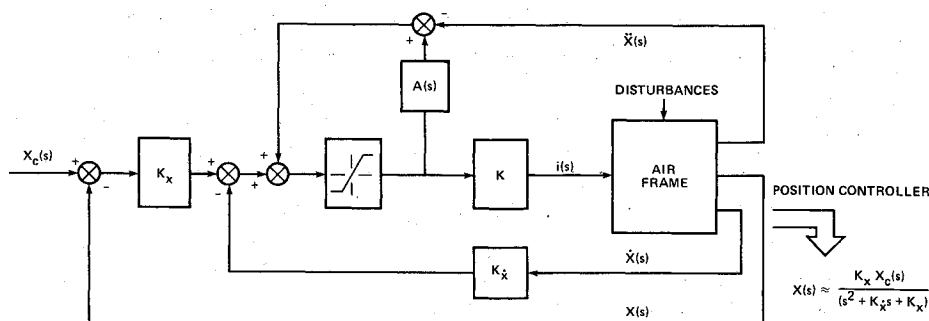


Fig. 3 Single-axis model-following controller.

Table 1 VSRA advanced control system

Force and moment producer	Actuator authorities and rates				Full control travel
	Series		Parallel		
Stabilator	+1.5, -1.5	60 deg/s	+7.5 deg, -4 deg	2.2 deg/s	12.7 deg, -11.7 deg
Pitch rcs ^a fwd	+29%, -29%	346%/s	100%, 0%	29%/s	7.3 in. ² , 0 in. ²
Pitch rcs aft	+19%, -19%	750%/s	69%, 0%	27%/s	8.7 in. ² , 0 in. ²
Ailerons	+2.0 deg, -2.0 deg	80 deg/s	+4.0 deg, -6.0 deg	2.0 deg/s	+12 deg, -27 deg
Roll rcs	+16%, -16%	760%/s	54%, -54%	9.6%/s	+ 8.1 in. ² , -8.1 in. ²
Rudder	—	—	—	—	+15 deg, -15 deg
Yaw rcs	+50%, -50%	500%/s	—	—	+3.5 in. ² , -3.5 in. ²
Thrust (psa) ^b	+5 deg, -5 deg	100 deg/s	75 deg, 0 deg	2.8 deg/s	75 deg, 0 deg
Nozzles	+5 deg, -5 deg	90 deg/s	98.5 deg, 2 deg	4.8 deg/s	98.5 deg, 2 deg

^arcs = reaction control system.

^bpsa = power spindle angle (same as throttle lever angle).

when the aircraft is hovering close to the ship's deck and superstructure. The simulated ship (a Spruance-class destroyer), as it is seen by the pilot on the computer-generated image from inside the cockpit, is shown in Fig. 5. The intersection of the diagonal lines on the ship deck marks the desired touchdown point.

To evaluate the hazardous effects of the failures, a failure rating scale (Fig. 6) was used by the pilots. The structure of this scale is based on a turbulence-effect rating scale presented in Ref. 7. The scale follows a format similar to that of the Cooper-Harper pilot rating scale,⁸ in that a dichotomous decision process leads to a narrowed choice of descriptors that categorize the ability to recover from a failure. The most critical question to be answered on this scale, for monitoring evaluation, has to do with whether safety of flight was compromised during the recovery. The answer to this question determines whether the failure was detected in time to allow a safe recovery.

The task flown during these failure evaluations was a curved decelerating approach from 120 knots to hover, starting at a point 2.7 n. mi. from the ship. The initial hover point, at the end of transition (Fig. 5), is 100 ft to port and aft of the ship at a gear altitude of 75 ft above the water. At this point, the pilot switches the control system from flight-path/longitudinal acceleration command (primary transition-control mode) to translational velocity command (hover-control mode) in all three axes. The pilot then translates the aircraft to the final hover point above the deck using the aircraft's head-up display for primary guidance and situation information. When over the ship, the gear height is nominally 43 ft above the landing pad (a 43 × 52 ft rectangle). The pilot then makes a vertical landing.

Computer malfunctions include hardware failures, coding errors, or any malfunction that causes the computer to issue an improper command. Failures simulated most often were computer commands that caused series-servo "hardovers." Control action following a hardover is shown by the bottom ("after-failure") time histories in Fig. 7. There are two important events in a hardover: the series servo saturates almost instantaneously, and then the parallel trim servo moves at a fixed rate in a direction intended to unload the series servo under normal operation. Both the stabilator and the aileron respond with nearly a step-displacement to the series-servo hardover, followed by a ramp with a slope equal to the parallel servo's trim rate. Note that the rudder has a zero slope after the initial jump, since the rudder does not have a parallel trim servo.

After a failure is detected, the control system is automatically switched to that of the YAV-8B with its SAS engaged. The series servo moves to the position commanded by the SAS, and the parallel servo remains at the value it reached at the time of failure detection (shown as "after reversion" in Fig. 7). Thus, the uncommanded control action during the failure has contributions from both servos, whereas after failure detection it is due only to the parallel servo. However, the flying-qualities effect of these control actions is reduced to some extent after

Table 2 VSRA command modes

Axis	Mode	
	Transition	Hover
Pitch	RC/AH	RC/AH
Roll	RC/AH	VC
Yaw	AC/TC	RC
Vertical	FPC	VC/alt hold
Longitudinal	AC/VH	VC
Command		Stabilization
RC: Rate command		AH: Attitude hold
AC: Acceleration command		TC: Turn coordination
FPC: Flight path command		VH: Velocity hold
VC: Velocity command		

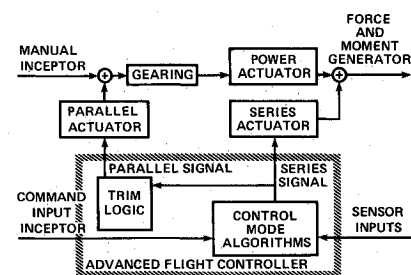


Fig. 4 Basic single-degree-of-freedom VSRA controller.

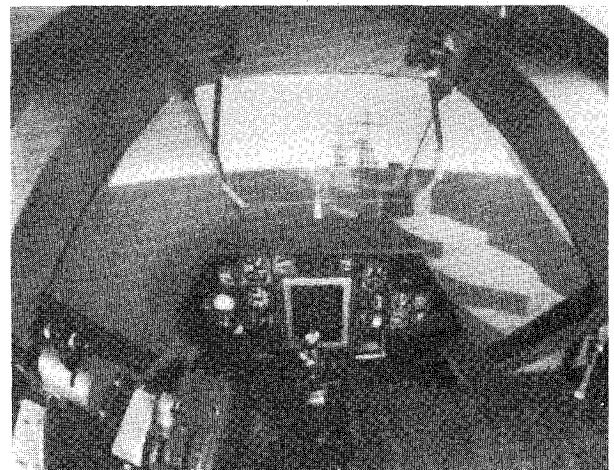


Fig. 5 Cockpit and visual scene.

reversion by the YAV-8B SAS acting through the attitude series servos.

To determine acceptable delays for failure detection in order to establish requirements for monitor performance, the time between failure injection and reversion (detected and performed by some hypothetical monitoring system) was varied. At reversion, an aural warning sounded in the pilot's headset. The pilot was instructed not to attempt a recovery until he heard the warning tone, even if he was able to detect the failure himself. In effect, the pilot's reaction time was controlled by the experimenter.

Attitude Servo Failure-Detection Requirements

The experimenter-controlled pilot reaction time was varied to establish the trend of the pilots' failure ratings, shown at the

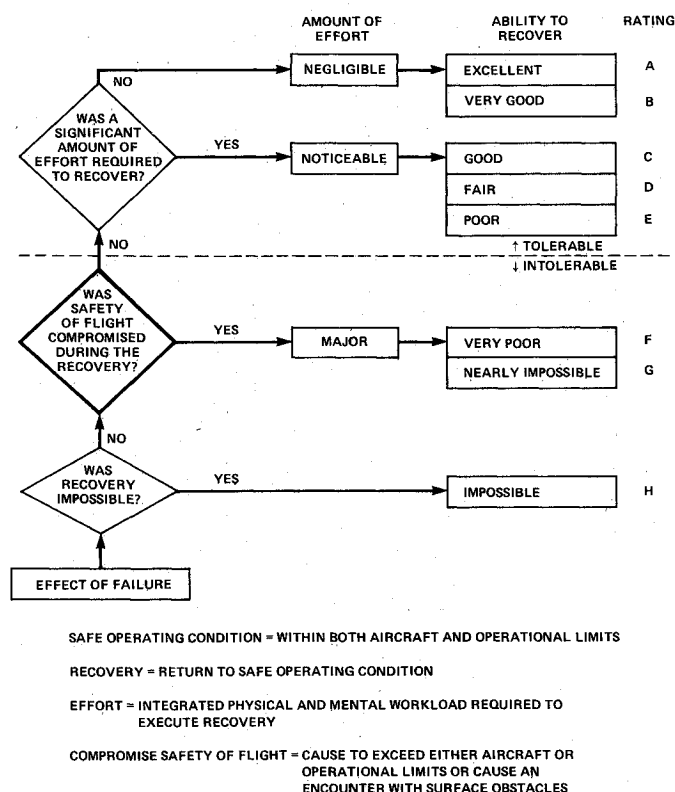


Fig. 6 Failure rating scale.

top of Fig. 7. Emphasis was given to the E to F portion of the rating scale, because this boundary defines the limit of system acceptability. From these data, it can be seen that for pitch-axis and roll-axis failures to receive ratings in the "tolerable" band, the detection time required must be less than or equal to approximately 0.8 s. A failure in the yaw axis never compromised safety of flight.

Throttle-Nozzle Servo Failure-Detection Requirements

Results similar in scope to those of Fig. 7 were also obtained for vertical (throttle) and the longitudinal (nozzle) failures; they are presented in Fig. 8. A more complete view of the problems associated with these failures is obtained from direct calculations founded on the test results. The results of these calculations illustrating the effects of vertical controller command failures are shown in Fig. 9. The graph depicts the combinations of system-plus-pilot-plus-engine reaction time, descent rate at the failure, and the altitude at the failure occurrence, which results in a touchdown at 9 ft/s. To prevent landing gear damage with the YAV-8B, touchdown velocities must be less than 12 ft/s. However, to provide a safety margin, pilots did not like to exceed 9 ft/s on touchdown. The right side of Fig. 9 shows the vertical accelerations used in the calculations of the accompanying curves. Initially, a failure occurs while the aircraft is descending at a constant rate. The effect of the failure is twofold. First, there is an acceleration of $0.08g$'s from the hardover of the series servo, and second, there is a time-varying acceleration of $0.043g \Delta t$ from the parallel servo attempting to center the series servo. Next in the sequence, the failure is detected, and the resulting vertical thrust is $T - 0.043g \Delta t$. The pilot now applies full power, which at the simulated weight corresponds to a thrust-to-weight ratio of 1.15. The final drawing in the sequence shows the aircraft touching down at the desired allowable maximum velocity.

From the figure, point A on the curve shows that if a vertical (thrust) command failure in the downward direction occurs at 13 ft above the deck while descending at 5 ft/s, and if the system-plus-pilot-plus-engine reaction time takes 1.5 s from failure to maximum thrust, then the aircraft will touch down at 9 ft/s. If the overall reaction time is longer than 1.5 s, then the monitoring system is not acceptable. Thus, the crosshatched region indicates the conditions allowable at the time of failure if 1.5 s is found to be the maximum system-plus-pilot-plus-engine reaction time. The nominal descent rate relative to the deck used in the simulation of the landing task was 3 ft/s. However, in the sea conditions under which the VSRA is designed to operate, the instantaneous rate of descent can exceed 4.5 ft/s. With the initial descent rate constraint, the maximum allowable time from failure to full thrust is 1.3 s. Allowing an engine spool-up time of 0.2 s means that the system-plus-pilot-

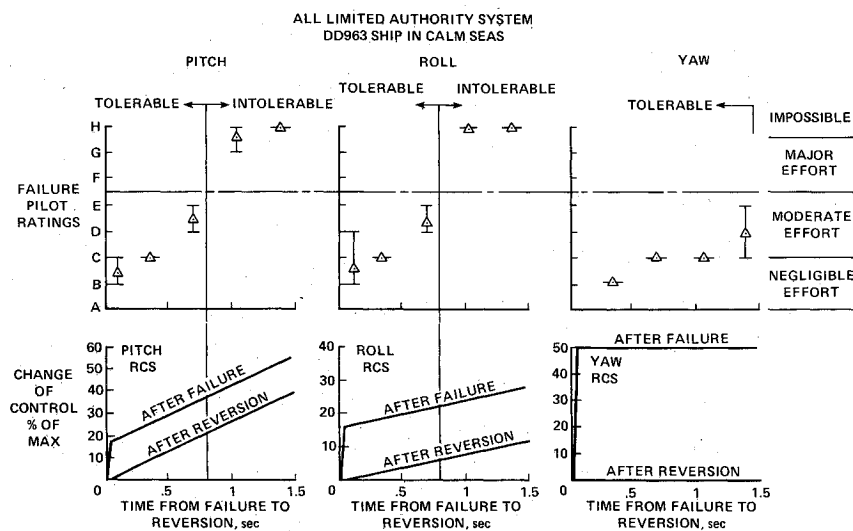


Fig. 7 Pitch, roll, and yaw hardover command failures at destroyer.

plus-engine reaction time must be less than 1.1 s. The test results shown in Fig. 8 agree closely with this result.

Figure 10 gives the calculated time from failure to final pitch attitude needed to prevent a nose boom contact with the ship's hangar door after a longitudinal controller (nozzle) command hardover failure. The distance of the YAV-8B's nose boom from a destroyer's hangar door when over the nominal touchdown point is 16 ft. In these calculations, it was assumed that at the time of reversion, the series servos were centered and that the pilot changed the pitch of the aircraft by an amount equal to twice the angle that the parallel servo had moved the nozzles through during the reaction time (this will initiate a deceleration equal and opposite to the acceleration caused by the movement of the parallel servo). This pitch angle, and therefore the deceleration, is maintained until the aircraft stops moving forward. Pilots always use pitch attitude to arrest accelerations caused by nozzle failures of small amplitudes, since it does not require a repositioning of the hands on the primary controls.

From Fig. 10, the upper bound of reaction time is 1.8 s, and the final incremental pitch attitude is 17 deg. The sequence at the right in Fig. 10 shows the aircraft experiencing the failure; the arrows show the thrust-vector inclinations relative to vertical. In the top drawing, the thrust vector is tilted forward 5 deg due to the series servo hardover. Next, the parallel servo further tilts the thrust forward linearly with time. In the third drawing, the failure is detected and the series servo has returned to center. The pilot now changes pitch attitude by twice the angle that the parallel servo trimmed the thrust vector forward during the failure. Finally, the forward translation is stopped. In hover, the pitch-control power of the aircraft (assuming the pitch damper becomes saturated immediately in the direction opposite to the recovery, leaving angular acceleration

command) is 0.6 rad/s^2 . Thus, the time required to reach the final pitch attitude of 17 deg is 1 s; therefore, the system-plus-pilot-plus-engine reaction time must be less than about 0.8 s. Test results shown in Fig. 8 agree closely with this result.

Monitoring System Description

Several control-command monitoring approaches were tried. A simple check for hardover failures is to examine how long a given servo has saturated. However, saturation of many of the research system's series servos occurs in normal operation during transition and landing, especially in a turbulent environment. The saturation time permitted before declaring a failure must be set large enough to prevent nuisance disconnects for saturations normally seen in flight, yet they must be set small enough to catch the effect of a hardover failure in time

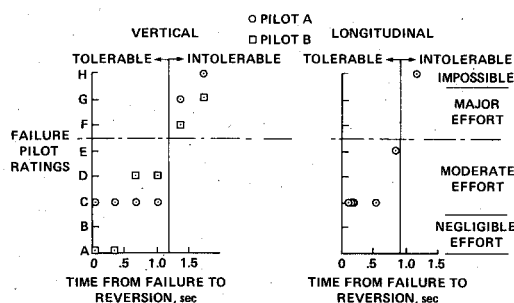


Fig. 8 Throttle/nozzle hardover command failures.

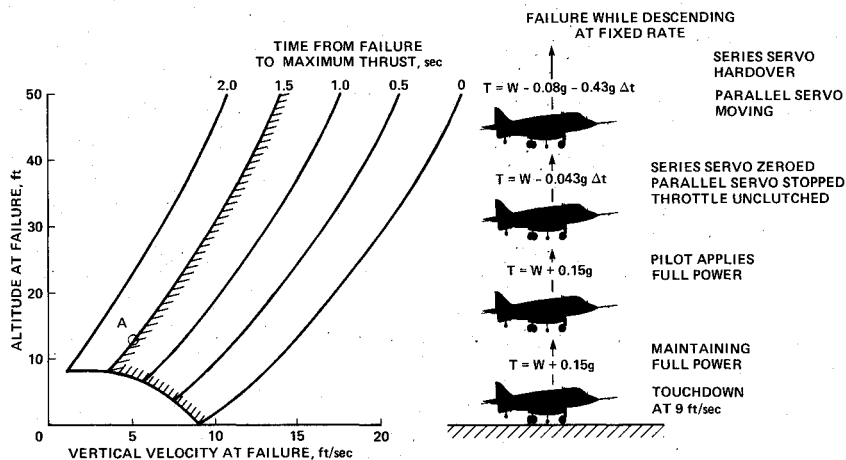


Fig. 9 Safe envelope for vertical (throttle) command failures.

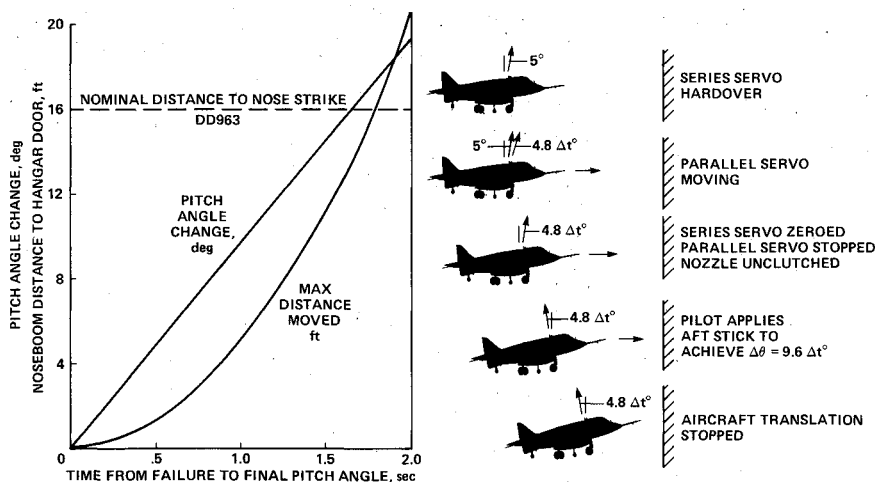


Fig. 10 Sample longitudinal (nozzle) command failures.

for the pilot to make a safe recovery. This method was successful only for the pitch and roll axes. Other axes would occasionally have longer series-servo saturation times in normal operation than could be allowed for in an adequate failure-detection time. A problem with this kind of monitoring scheme is that it is only applicable to hardovers. The scheme is totally ineffective for slow failures and, in particular, for failures that cause the servo to freeze at a given position.

A flight-envelope monitoring scheme was also tried. Here, a linear functional of the states and state rates is used to define a "normal" operating flight envelope. If the functional exceeds a preset value, it is assumed that a failure has taken place, and control is switched to the YAV-8B system with its production SAS operating. For example, for height control in hover, it is reasonable to use the weighted sum $K_1\dot{h} + K_2\ddot{h}$ to monitor the vertical axis. The conjecture is that if the sum exceeds an envelope limit as a function of altitude, a failure has probably occurred. The problem with this scheme is that failures can only be detected quickly enough if the functional is made heavily dependent on measured acceleration. Unfortunately, such a functional tends to provide a very restrictive operational envelope and is sensitive to disturbances. The monitor is prone to disconnects in the descent over the ship where there is little maneuvering, but where ship air-wake turbulence is high. This monitoring method could not be made to work satisfactorily.

The monitoring system that was finally used is based on the following idea. Since the VSRA is designed to follow a simple dynamic model, why not compare the aircraft's response to a pilot's input with that of the simple dynamic model itself? (In an explicit model-following system, this simple dynamic model signal would be available explicitly.) For example, the model dynamics desired to be followed for longitudinal velocity commands in hover are

$$(V_m/V_c) = [1.75^3/(s + 1.75)^3]$$

where s is the Laplace transform variable, V_m is the model's velocity response, and V_c is the pilot's commanded velocity. The pilot's velocity command inputs are simultaneously sent to the primary flight computer and to the monitor computer. The latter calculates the response of the simple transfer function model of the desired dynamics indicated above. The absolute value of the difference between the resulting longitudinal velocity of the aircraft and the desired modeled velocity (output of the simple transfer function model) is compared in the monitor computer with a preset value. If the difference exceeds the preset value, then, for whatever reason, the aircraft is not following the desired dynamics, and a failure is assumed to have occurred. Since the implicit model-following system is self-trimming, no steady-state bias exists between the command and the desired aircraft motion. Thus, the desired model outputs will not require adjustment to account for a steady-state error buildup, and the model-following error, when tested against the preset value, will not be contaminated with a steady-state error. Both of these results minimize nuisance disconnects. The primary advantages inferred for this "model comparator" monitor are 1) independence of the measured aircraft acceleration, with less sensitivity to turbulence, hence tighter detection tolerances and quicker detection times, and 2) slow failures should be detected quickly, since model comparators use the pilot's input, as well as the aircraft's state to determine the system's integrity. A potential disadvantage is that a change in the desired aircraft response will require a change to the monitor software, so that the monitor is not truly independent of the control laws as is, for example, the flight-envelope monitor. It follows that care must be exercised to maintain its integrity.

The extent to which the aircraft can follow the desired dynamics depends on several factors, perhaps the most important of which is the response of the aircraft to external disturbances. In the simulation, disturbances become severe when the aircraft descends behind the destroyer's superstructure. Uncom-

manded motions caused by disturbances appear as errors in model tracking. The command-following tolerances must be set large enough to withstand these disturbance-induced errors.

With the system mechanization described, the ability of the aircraft either to follow large input maneuvers or regulate properly against large disturbances depends on the authorities of the series servos and the rates at which the parallel servos can center these series servos. Anytime a system command causes the series servos to saturate for any period of time, the system can no longer accurately follow the desired simple linear model. This accuracy is governed by the trim rate of the parallel servos.

An example, in hover, of the accuracy of the model-following in the simulation is shown in Fig. 11. Shown here, for a typical landing, are the pilot's longitudinal velocity command input, the aircraft's true velocity response, the desired model's velocity response, the difference between the desired and the actual velocity response, the position of the nozzle series servo, and the nozzle angle. The difference between the desired and the actual velocity response, which is less than 0.3 ft/s, is monitored for control-system integrity. At approximately 40 s into the run, a nozzle series-servo failure occurs, which causes the actual horizontal velocity to diverge from the desired velocity. When the velocity error exceeds the preset error tolerance (1.2 ft/s), the failure is detected.

The monitor models for each axis and the error tolerances determined from simulation are given for both hover and transition in Tables 3 and 4. These error tolerances were found experimentally through an iterative process. First, maximum single-axis pilot command inputs were injected into the system in a turbulent environment; the errors noted were used as the initial tolerances. Then, failures were injected; if the detection time was less than that determined from the monitor-system-requirements simulation, the monitor was adequate. If the desired detection time was greater than required, the error tolerance was reduced until the desired failure-detection time could be met. However, this process lowers the maneuverability for that degree of freedom. The error tolerances were then fine-tuned against nuisance disconnects by hovering behind the ship's superstructure in a moderate sea state (sea state 4). If a false trip occurred due to a disturbance, then the error tolerance was increased.

It may be seen from Table 4 that the smallest propulsion system monitor tolerance is the 1.2 ft/s for the longitudinal velocity command monitor. A monitor trip level this small raises the question of whether or not the velocity can be measured with sufficient accuracy to avoid excessive nuisance disconnects. Velocities measured by the IMU's have an rms error of 2.5 ft/s. It is expected to be able to reduce this error by an

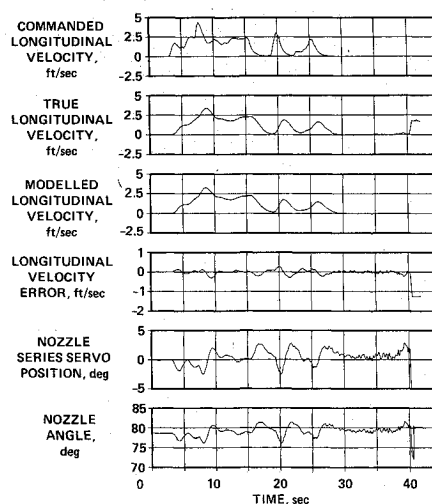


Fig. 11 Longitudinal velocity command system and monitor performance: shipboard landing.

Table 3 Attitude monitors

		Axis		
Mode		Pitch	Roll	Yaw
Model	Transition	$\frac{\theta_m}{\theta_c} = \frac{2^2}{(s+2)^2}$	$\frac{\phi_m}{\phi_c} = \frac{2^2}{(s+2)^2}$	none
	Hover	$\frac{\theta_m}{\theta_c} = \frac{2^2}{(s+2)^2}$	$\frac{\phi_m}{\phi_c} = \frac{2^2}{(s+2)^2}$	$\frac{\dot{\psi}_m}{\dot{\psi}_c} = \frac{4}{s+4}$
Disconnect condition	Transition	$ \theta - \theta_m > 1 \text{ deg}$	$ \phi - \phi_m > 12 \text{ deg}$	none
	Hover	$ \theta - \theta_m > 0.4 \text{ deg}$	$ \phi - \phi_m > 1.2 \text{ deg}$	$ \dot{\psi} - \dot{\psi}_m > 5 \text{ deg/s}$

Subscript c = Pilot command; m = Model response.

Table 4 Propulsion system monitors

		Axis	
Mode		Longitudinal (nozzle)	Vertical (throttle)
Model	Transition	$\frac{V_m}{V_c} = \frac{1}{s} - \frac{s}{(s + 1.75)^2}$	$\frac{\gamma_m}{\gamma_c} = \frac{0.88}{(s + 0.88)}$
	Hover	$\frac{V_m}{V_c} = \frac{1.75^3}{(s + 1.75)^3}$	$\frac{\dot{h}_m}{\dot{h}_c} = \frac{7 \cdot 0.88}{(s + 7)(s + 0.88)}$
Disconnect condition	Transition	$ V - V_m > 8 \text{ ft/s}$	$ \gamma - \gamma_m > 3 \text{ deg}$
	Hover	$ V - V_m > 3 \text{ ft/s } (h > 30 \text{ ft})$ $ V - V_m > 1.2 \text{ ft/s } (h \leq 30 \text{ ft})$	$ \dot{h} - \dot{h}_m > 3 \text{ ft/s } (h > 30 \text{ ft})$ $ \dot{h} - \dot{h}_m > 1.5 \text{ ft/s } (h \leq 30 \text{ ft})$

Subscript c = Pilot command; m = Model response.

Table 5 Monitor performance: hover

Axis	Performance required monitor time delay, s	Performance achieved monitor time delay, s	Performance achieved failure rating
Pitch	0.8	0.32	B
Roll	0.8	0.35	B
Yaw	not critical	1.00	C
Vertical	1.2	0.90	D-E
Longitudinal	0.9	0.42	D

order of magnitude by complementary filtering, using aircraft position from a ground-based laser tracker. The resulting rms error of 0.25 ft/s should be acceptable, since it is anticipated that most of this error will be at the 84 min Schuler period, and will, therefore, vary slowly enough to be compensated by the self-trimming feature of the control system. Protection against excessive low-frequency and bias errors, which will not be caught by the response monitors, will be provided by the sensor monitors.

Monitoring System Results

Once all the tolerances had been set, a series of landings was performed, failures injected, and failure ratings taken. With the final monitor design, 105 computer command and servo failures were injected during both hover and transition. These tests covered single and multiple servo failures that were either hardover or passive. The experimenters used experience gained, as the tests proceeded, to create conditions requiring the most demanding recovery actions from the pilot. A composite of the failure results is shown on the histogram in Fig. 12. It can be seen that no computer command failure caused safety of flight to be an issue. In addition, no nuisance disconnects occurred during the piloted evaluations when the pilot was performing the landing tasks. Pilots could cause the system

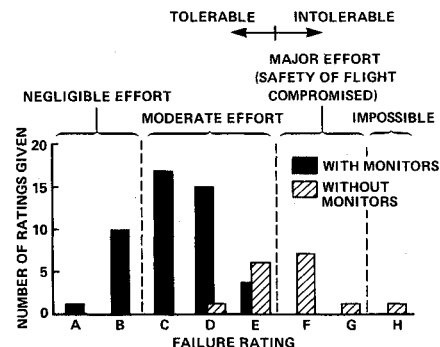


Fig. 12 Reverting to YAV-8B with SAS following computer command failures in hover (hardovers and holds).

to nuisance disconnect if large authority step inputs were attempted.

Figure 12 also shows results for failures that were injected without a monitoring system. In these cases, the pilot detected the failure and initiated the reversion. The pilot had to detect the failure either visually, by the motion cues, or by the unusual behavior of the back-driven controls. Most of the failures

shown caused safety of flight to be compromised during the recovery, which is unacceptable. These results clearly prove that a monitoring system is required in the flight environment.

Failures injected during the transition task (120 knots to hover) were all recoverable, with ratings better than D. Since plenty of altitude was available for recovery in the transition task, and adequate margins existed from flight-envelope boundaries, safety of flight was never an issue.

An axis-by-axis breakdown of the final monitoring system's performance is given in Table 5. Maximum detection times during the evaluations with the model comparator monitors may be compared with the maximum acceptable disconnect times obtained in the simulation to obtain the monitoring system requirements. All requirements were met with conservative margins in all cases.

Conclusions

A control system monitoring scheme has been evaluated in a manned moving-based simulation to investigate the effects of control-system failures in NASA's V/STOL Research Aircraft. Failures of the aircraft's control system during simulated landings on a Spruance-class destroyer showed that the model comparator monitor detected and disengaged the failed control system in time to permit a safe recovery. Furthermore, the monitor did not overly restrict maneuverability for the landing task on a destroyer-sized ship, and nuisance disconnects were minimal. The tests verified that the monitor was insensitive to

external disturbances, and that it was equally effective at detecting both fast and slow failures.

References

- ¹Ammons, E. E., "F-16 Flight Control System Redundancy Concepts," AIAA Paper 79-1771, 1979.
- ²Kelly, J. R., Niessen, F. R., Garren, J. F., and Abbott, T. S., "Description of the VTOL Approach and Landing Technology (VALT) CH-47 Research System," NASA TP-1436, 1979.
- ³Holden, D. G., "HOME—An Application of Fault Tolerant Techniques and System Self-Testing," *IEEE Intercon Conference Record*, Paper 11/2, 1975.
- ⁴Bradbury, P., "Augmentor Wing STOLAND Servo and Monitoring Summary," Sperry Flight Systems, Phoenix, AZ, Rept. 5440-0222-A445, 1974.
- ⁵Moralez, E., Schroeder, J. A., and Merrick, V. K., "Simulation Evaluation of the Advanced Control System Concept for the NASA V/STOL Research Aircraft (VSRA)," AIAA Paper 87-2535-CP, 1987.
- ⁶Merrick, V. K., "Study of the Application of an Implicit Model-Following Flight Controller to Lift Fan VTOL Aircraft," NASA TP-1040, 1977.
- ⁷Lebacqz, J. V. and Aiken, E. W., "A Flight Investigation of Control, Display, and Guidance Requirements for Decelerating Descending VTOL Instrument Transitions Using the X-22A Variable Stability Aircraft," Naval Air Systems Command, Rept. AK-5336-F-1, Sept. 1975.
- ⁸Cooper, G. C. and Harper, R. P., "The Use of Pilot Rating in the Evaluation of Aircraft Handling Qualities," NASA TN-D-5153, 1969.

Recommended Reading from the AIAA Progress in Astronautics and Aeronautics Series . . .



Numerical Methods for Engine-Airframe Integration

S. N. B. Murthy and Gerald C. Paynter, editors

Constitutes a definitive statement on the current status and foreseeable possibilities in computational fluid dynamics (CFD) as a tool for investigating engine-airframe integration problems. Coverage includes availability of computers, status of turbulence modeling, numerical methods for complex flows, and applicability of different levels and types of codes to specific flow interaction of interest in integration. The authors assess and advance the physical-mathematical basis, structure, and applicability of codes, thereby demonstrating the significance of CFD in the context of aircraft integration. Particular attention has been paid to problem formulations, computer hardware, numerical methods including grid generation, and turbulence modeling for complex flows. Examples of flight vehicles include turboprops, military jets, civil fanjets, and airbreathing missiles.

TO ORDER: Write AIAA Order Department,
370 L'Enfant Promenade, S.W., Washington, DC 20024

Please include postage and handling fee of \$4.50 with all orders.
California and D.C. residents must add 6% sales tax. All foreign orders
must be prepaid. Please allow 4-6 weeks for delivery. Prices are subject
to change without notice.

1986 544 pp., illus. Hardback
ISBN 0-930403-09-6
AIAA Members \$54.95
Nonmembers \$72.95
Order Number V-102